Environ Earth Sci
DOI 10.1007/s12665-013-2462-4

ORIGINAL ARTICLE

Estimation of net primary productivity using a process-based model in Gansu Province, Northwest China

Peijuan Wang · Donghui Xie · Yuyu Zhou · Youhao E · Qijiang Zhu

Received: 27 November 2012 / Accepted: 26 March 2013

Abstract The ecological structure in the arid and semi-arid region of Northwest China with forest, grassland, agriculture, Gobi, and desert, is complex, vulnerable, and unstable. It is a challenging and sustaining job to keep the ecological structure and improve its ecological function. Net primary productivity (NPP) modeling can help to improve the understanding of the ecosystem, and therefore, improve ecological efficiency. The boreal ecosystem productivity simulator (BEPS) model provides the possibility of NPP modeling in terrestrial ecosystem, but it has some limitations for application in arid and semi-arid regions. In this paper, we improve the BEPS model, in terms of its water cycle by adding the processes of infiltration and surface runoff, to be applicable in arid and semi-arid regions. We model the NPP of forest, grass, and crop in Gansu Province as an experimental area in Northwest China in 2003 using the improved BEPS model, parameterized with moderate resolution remote sensing imageries and meteorological data. The modeled NPP using improved BEPS agrees better with the ground measurements in Qilian Mountain than that with original BEPS, with a higher R^2 of 0.746 and lower root mean square error (RMSE) of 46.53 gC m^{-2} compared to R^2 of 0.662 and RMSE of 60.19 gC m^{-2} from original BEPS. The modeled NPP of three vegetation types using improved BEPS shows evident differences compared to that using original BEPS, with the highest difference ratio of 9.21 % in forest and the lowest value of 4.29 % in crop. The difference ratios between different vegetation types lie on the dependence on natural water sources. The modeled NPP in five geographic zones using improved BEPS is higher than those with original BEPS, with higher difference ratio in dry zones and lower value in wet zones.

Keywords Net primary productivity · Arid and semi-arid regions · BEPS

Introduction

Vegetation is one of the most important assimilators of carbon dioxide in terrestrial ecosystems. It plays an important role in global matter and energy cycle, carbon balance, and climate change. Plants assimilate carbon dioxide in the atmosphere and incorporate it into the biomass through photosynthesis, and part of the assimilated carbon is emitted into the atmosphere through plant respiration (autotrophic respiration). The difference between accumulative photosynthesis and accumulative autotrophic respiration by green plants per unit time and space is defined as net primary productivity (NPP) (Leith and Whittaker 1975).

It has been a popular method to estimate regional NPP using models. NPP models can be classified into three types: statistical models, parameter models, and process-based models. Statistical models, such as the Miami model

P. Wang (✉) · Y. E
Chinese Academy of Meteorological Sciences, Beijing 100081, China
e-mail: wangpj@cams.cma.gov.cn

D. Xie · Q. Zhu
State Key Laboratory of Remote Sensing Science, Jointly Sponsored by Beijing Normal University and Institute of Remote Sensing Applications of Chinese Academy of Sciences, Beijing 100875, China

Y. Zhou
Joint Global Change Research Institute, 5825 University Research Court, Suite 3500, College Park, MD 20740, USA

Published online: 16 April 2013

and Thornthwaite Memorial model (Leith and Whittaker 1975), estimate NPP by establishing the statistical relationship between NPP and climate data. Though these models show simplicity in NPP modeling, they can only estimate the potential NPP but not the real NPP. Parameter models, such as CASA, calculate NPP through the energy conversion efficiency and the solar radiation absorbed by vegetation (Potter et al. 1993). Because the parameter models lack certain critical ecological processes using empirical relationship and constant (e.g. light-use efficiency) (Matsushita et al. 2004), they cannot explain NPP theoretically and further limit their applications. Process-based models are built based on physiological and ecological processes. Photosynthesis, evapotranspiration, autotrophic respiration, and dry matter partition are considered when estimating NPP in the process-based models, such as FOREST-BGC (Running and coughlan 1988), BIOME-BGC (Hunt and Running 1992), IBIS (Foley et al. 1996), and BEPS (Liu et al. 1997, 1999, 2002; Chen et al. 1999). In northern China, water plays a dominated role not only in the distribution of vegetation but also in the rate of change in the vegetated area (Zhang and Zhou 2011). Especially in northwest China, water can fatally influence crop productivity (Liu et al. 2011b) and exacerbate the vulnerable eco-environment (Zhou et al. 2011). Even in southwestern China, such as Guizhou province, the vegetation NPP in some less precipitation areas strongly depends on the available water content (Wang et al. 2010). Generally, those above models considered vertical movement of rainfall from top to bottom when simulating water cycling processes of land ecosystem. However, if the effective rainfall is less than ecological water requirement of vegetation, these process-based models may have some limitations in the simulation of NPP, especially in complex terrain (Soulis et al. 2000). It will underestimate soil moisture content without the mechanistic horizontal redistribution of soil water under the assumption of good surface infiltration capacity (Ju et al. 2006).

Efforts had been attempted to build a distributed hydrological model by considering the influence of the lateral water flow in the simulating the detailed spatial and temporal variation patterns of evapotranspiration (ET) (Chen et al. 2005). Although this improved model had been applied to estimate the ET in a small watershed in Saskatchewan, vegetation NPP was not simulated by coupling three-dimension hydrological model. A coupled terrestrial carbon and hydrological model (BEPS-TerrainLab model) was developed to evaluate the topographic effects on NPP in Baohe River basin, Shaanxi Province, northwest China (Chen et al. 2007). The results showed that the average NPP was overestimated by 5 % without consideration of the topographic effects on the distributions of climatic variables and ground water movement.

In order to understand the impact of horizontal redistribution of soil water on vegetation NPP in arid and semi-arid region, Gansu Province in Northwest China is selected for NPP modeling by considering the three-dimension hydrological cycle in this paper. It is organized in four sections following this introduction: "Study area" gives a description of the study area; "Data and methods" details the key input parameters, and introduces the approach to improve the BEPS model according to the characteristics of arid and semi-arid regions; "Results and discussion" validates the modeled NPP with field measurements and other modeled NPP, compares the modeled NPP using original and modified BEPS, and analyses the spatio-temporal patterns of NPP; The last section summarizes the conclusions of this paper, and some limitations are also discussed in the end of this paper.

Study area

According to geographical and climatic characteristics, Gansu Province in northwest China, an arid and semi-arid region, is ideal to test the BEPS model with the capability of three-dimension hydrological representation. It was selected to study the vegetation NPP by considering the influence of lateral water flow based on the modified BEPS model using meteorological data and remotely sensed imageries. It will help to improve comprehension and evaluation of ecological efficiency in arid and semi-arid regions in Northwest China.

Gansu province lies in the Northwest China with the terrain tilting from southwest to northeast. It is 1,600 km in east–west direction and 530 km in north–south direction. The total area is about 455,000 km^2, roughly 4.7 % of total area of China. The study area is influenced by a temperate continental climate, with warm to hot summers and cold to very cold winters. The annual average air temperature is between 0–14 °C, and the annual average precipitation varies greatly from place to place between 42–760 mm, with a decreasing trend from southeast to northwest. Most of the precipitation is delivered in the summer months. The sunlight is about 1,700–3,300 h annually, increasing from southeast to northwest.[1] Every ten-day average temperature and precipitation in 28 stations from January 1st 1960 to December 31st 2010 were calculated and interpolated with inverse distance weighted (IDW) method. The spatial patterns of annual average temperature and precipitation in Gansu province are shown in Fig. 1. From Fig. 1 we can see that lower temperature regions mainly locate in northwest for its high latitude and southeast for its high

[1] Source: Ministry of Commerce of the People's Republic of China Website (http://english.mofcom.gov.cn/aroundchina/Gansu.shtml).

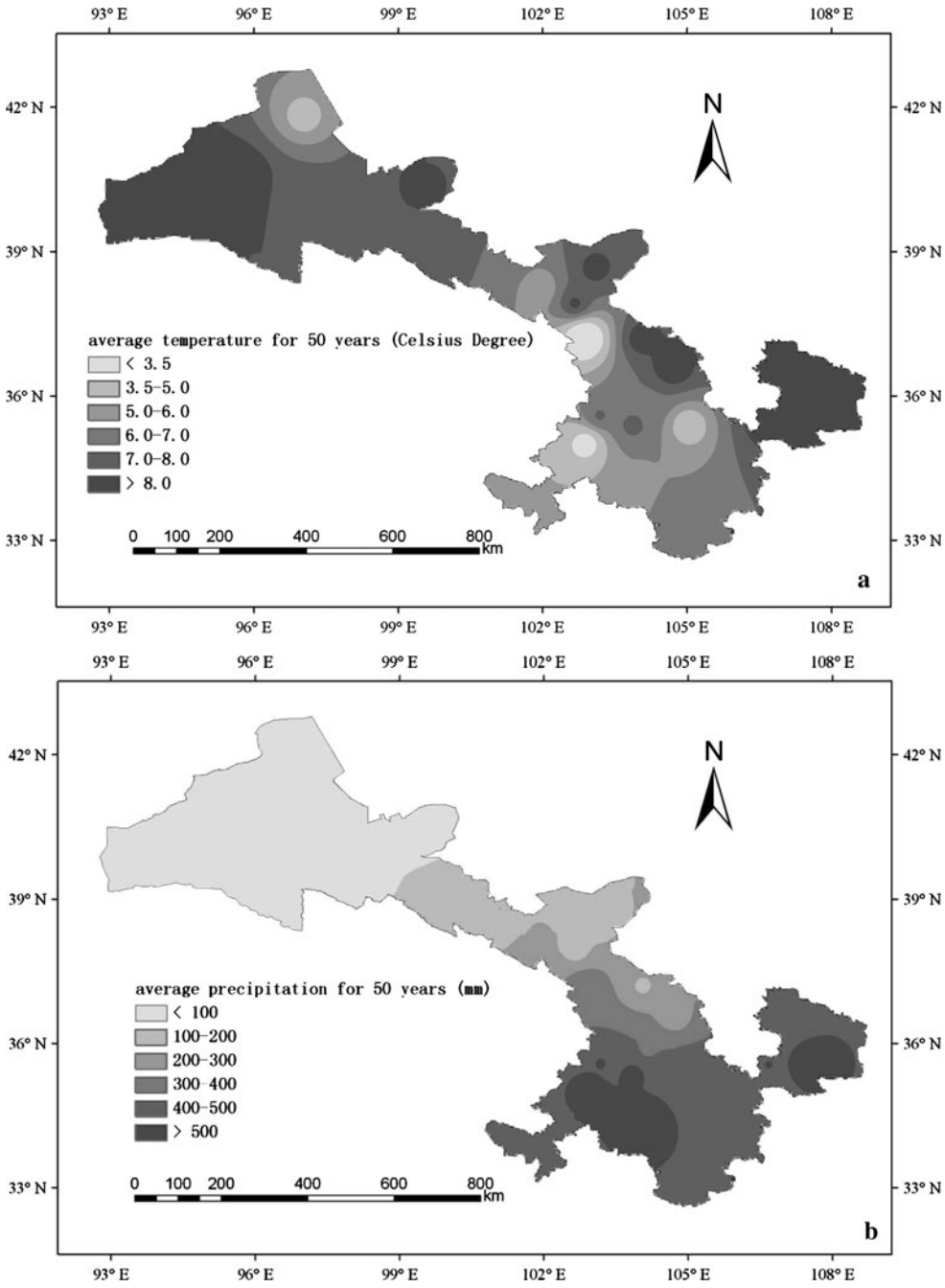

Fig. 1 Spatial patterns of annual average temperature (**a**) and precipitation (**b**) in Gansu province

altitude. For the precipitation, obvious distribution pattern related with latitude has been taken on. There is little precipitation in high latitude regions and much in low latitude areas.

The landscape is complex and diverse in Gansu province, including mountains, plateaus, plains, river valleys, deserts, and Gobi in staggered distribution Source: Ministry of Commerce of the People's Republic of China Website (http://english.mofcom.gov.cn/aroundchina/Gansu.shtml), with an elevation higher than 1,000 m in most of the areas. The vegetation types vary with altitude and slope, forming a vertical distribution of the desert—grass—forest structure with the increasing of DEM. The land cover is derived based on remote sensing images, vegetation distribution, and land use survey data in 2000. The types include crop, forest, grass, water, urban, and others. The spatial distribution of land cover types and DEM in Gansu province is shown in Fig. 2.

For better understanding the spatial patterns of NPP in Gansu province, we grouped Gansu Province into 5 zones according to geographical landscape features and climatic conditions, including climate, land cover, and topographical conditions. They are Hexi Corridor and northern Mountains,

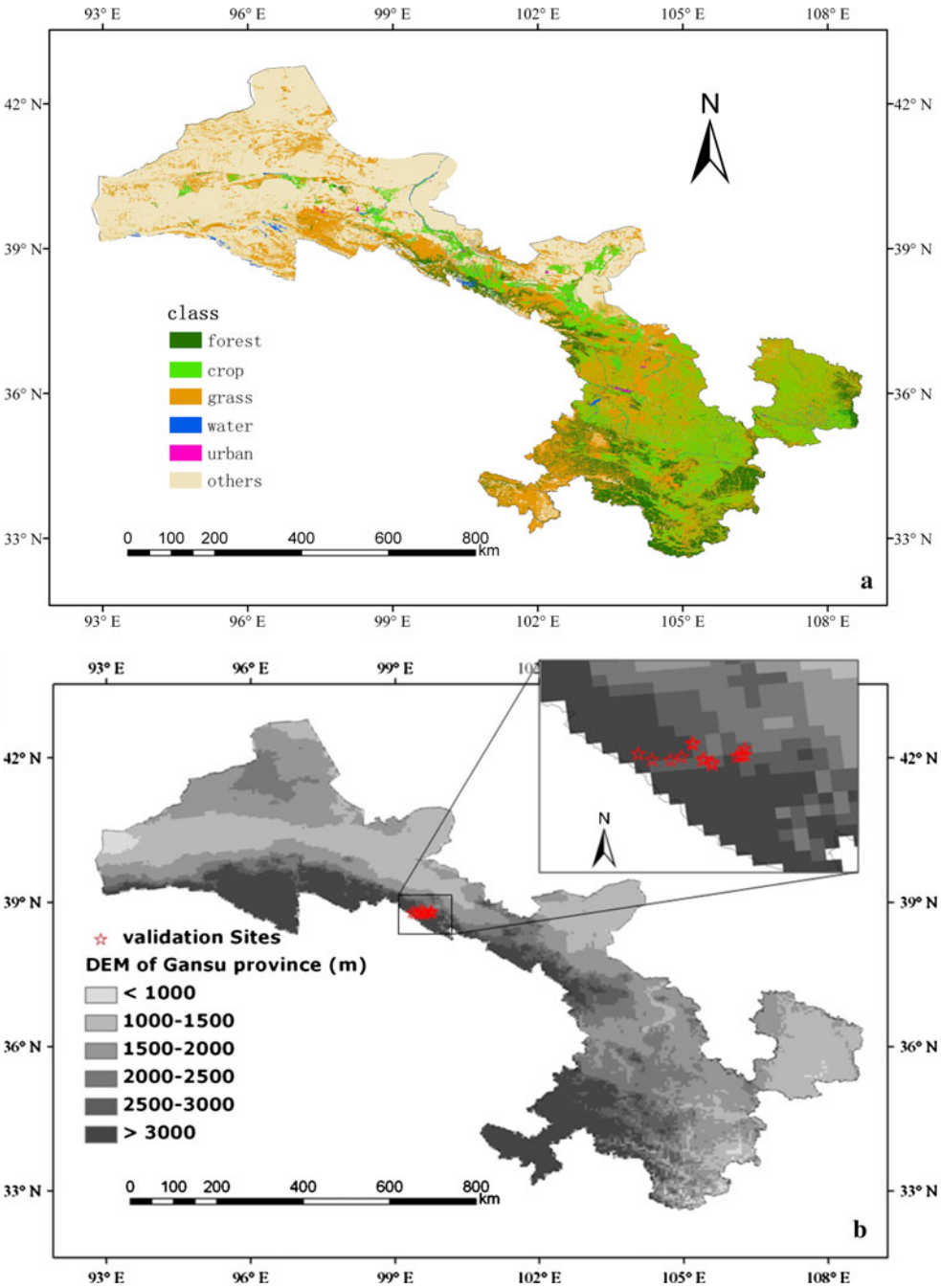

Fig. 2 Spatial distribution of land cover (**a**) and DEM (**b**) in Gansu province. In **b**, the upper-right picture is zoomed in region for 14 validation sites

Qilian Mountain, middle Loess Plateau, southern Mountain, and southern Plateau (Fig. 3). The descriptions about 5 zones are detailed in the followings[2] (Liu 2010).

Hexi Corridor and northern Mountains, located in the northern part of Gansu Province, is a long and narrow zone from northwest to southeast. The elevation varies from 1,000 to 1,500 m. The climate is dry and cold, and the sunshine is abundant.

Zone of Qilian Mountain lies in the western part of Gansu Province, the southern wing of Hexi Corridor. Altitude in most area is more than 3,500 m and the temperature is low. Influenced by climate and terrain, vegetation distribution shows clear vertical distribution. This zone is dominated by water conservation forest, and *Picea crassifolia* is the typical vegetation in this region.

Middle Loess Plateau locates in the eastern part of Gansu Province, which is a basined plateau. The temperature is low, and spatial–temporal variability of

[2] Refer to: Baidu (http://baike.baidu.com/view/8461.htm) and Wikipedia (http://en.wikipedia.org/wiki/Gansu).

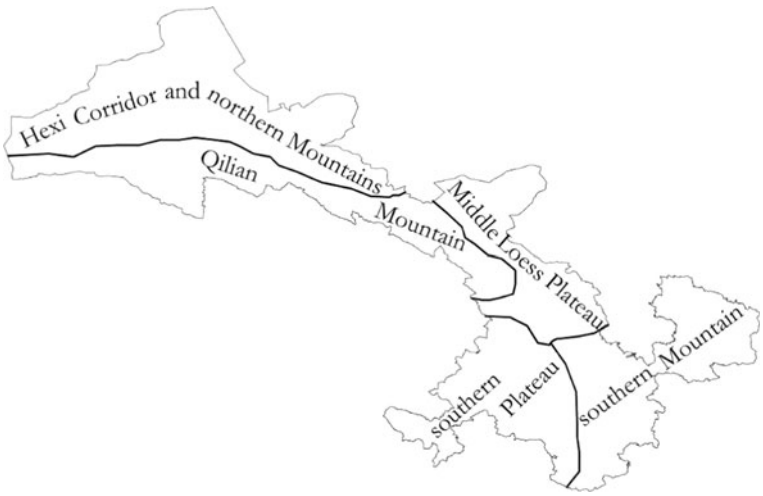

Fig. 3 Zonal map in Gausu Province

precipitation is high. Vegetation coverage is low in this area for loose soil structure and low nutrient content.

Southern Mountain is the westward extension of Qinling Mountains. It belongs to temperate and sub-humid areas, where resources of water and forest are abundant.

Southern Plateau lies in the eastern part of the Qinghai-Tibetan Plateau with an average altitude of over 3,000 m. It is wet and cold being affected by the Mongolian anticyclone and continental cyclones.

Data and methods

Data

The major data used in this study include multi-temporal LAI, meteorological data, and available water capacity (AWC) data. Both meteorological and soil data are gridded in the same resolution and map projection as remote sensing inputs. The descriptions about the data are detailed in the followings:

Multi-temporal LAI data

The multi-temporal leaf area index (LAI) data are one of the most important inputs for both original and modified BEPS models. We used MODIS 8-day LAI products (MOD15A2) at 1-km spatial resolution in 2003 for NPP simulation in this study. Meanwhile, multi-temporal LAI data from 2002 to 2010 were used to model vegetation NPP for spatial and seasonal analysis. All these data were projected to Albers Conical Equal Area (ACEA) projection.

Meteorological data

Ten-day meteorological data at 28 observed stations, including maximum average temperature, minimum average temperature, average relative humidity, and total precipitation, were retrieved from National Meteorological Information Center in China (http://mdss.cma.gov.cn:8080). Gap value was filled with the average of neighboring 2 days for temperature and humidity, and precipitation was filled with zero. After that, all meteorological factors were interpolated using IDW method to build gridded maps with same spatial resolution as LAI inputs.

The solar radiance was calculated using latitude, elevation, average relative humidity, maximum average temperature, minimum average temperature, and average temperature using Winslow's method (Winslow et al. 2001):

$$R_s = \tau_{cf} D(1 - \beta h^{T_{max}}) Q_0 \quad (1)$$

where R_s is daily solar irradiance at the earth's surface; τ_{cf} is cloud-free atmospheric transmissivity; D is day-length correction; $(1 - \beta h^{T_{max}})$ is the drop in relative humidity over the course of the day, where $h^{T_{max}}$ is the relative humidity at the time of maximum temperature, and β is a parameter varied with the sites, which can be described as $\beta = \max\{1.041, 23.753 \times \Delta T/(T_{mean} + 273.16)\}$, where ΔT is the mean annual temperature range between T_{max} and T_{min}, and T_{mean} is the average temperature; Q_0 is the total daily solar radiation incident at the top of the atmosphere. All those parameters can be calculated from the basic meteorological data and geographical data mentioned above.

AWC data

The AWC data were obtained by digitalizing the soil texture map and building the relationship between soil textures and soil water constant (Zhou et al. 2005).

Methods

An overview of BEPS

BEPS model was built on a processed model, FOREST-BGC (Running and Coughlan 1988). The biological, ecological, and hydrological principles are adopted for modeling the processes governing carbon and water flows in the soil–plant–atmosphere system. BEPS is composed of four sub-models, including canopy radiation sub-model, carbon cycling sub-model, water cycling sub-model, and physiological adjustor sub-model (Liu et al. 1997, 2002). In recent years, BEPS was successfully used to simulate NPP in different regions of East Asia with different spatial resolution, such as in East Asia region with 1 km resolution (Matsushita and Tamura 2002), whole China with 1 km resolution (Feng et al. 2007), and Changbaishan Natural Reserve and Dunhua county in Northern China with 30 m resolution (Wang et al. 2007) and Qilian Mountain in Northwest China with 15 m resolution (Zhou et al. 2007). Meanwhile, the canopy radiation sub-model was modified due to accidented terrain in Changbaishan Natural Reserve in China (Wang et al. 2006), whose improvement has also been used in this study.

Modification of BEPS model in Northwest China

The processes of water cycling are modeled considering rainfall, canopy interception, snowmelt, sublimation, evaporation, transpiration, and surface runoff in original BEPS water cycling sub-model. Rainfall is the major parameter in this sub-model. When it is raining or snowing, parts of them are intercepted by canopy to vaporize or sublimate, and others flow or melt into the soil to be used by vegetation. When the precipitation is greater than the largest water demand of vegetation, parts water will infiltrate into the soil, and the excess water will flow into the soil surrounding areas by surface runoff and subsurface flow.

Two hypotheses were made when modeling water cycling in original BEPS model. One is that the soil has a high surface infiltration capacity, and the other one is that surface runoff does not occur until the whole soil profile is saturated at the computational time step. Thus, excess rainfall goes into the soil through infiltration. Meanwhile, surface runoff is so small as to be negligible. Some limitations may exist for above assumptions. The soil surface infiltration beneath forest vegetation is low in the mountains for its critter crust (Zhang et al. 2011) and petrous soil, especially in arid and semi-arid mountain areas with coniferous forest in Northwest China. Thus, infiltration and surface runoff may happen simultaneously when precipitation occurs. Therefore, the assumptions in water cycle sub-model of original BEPS may be biased in arid and semi-arid region in Northwest China, and improvement is necessary for the NPP simulation.

Because of large relative altitude in mountain areas, available water in forest vegetation comes from not only vertical precipitation over land surface but also surface runoff in surrounding areas (Fig. 4). Evapotranspiration and evaporation processes were modeled in the original BEPS by a modified Penman–Monteith formula. The processes of surface runoff and infiltration were not considered in the original BEPS model as mentioned. To overcome this shortcoming, the water cycling sub-model in the BEPS was improved by adding the processes of surface runoff and infiltration to account for complex processes under accidented terrain.

1. Infiltration process

The surface infiltration is related to not only rainfall intensity but also soil texture and available water content. Based on different surface experiments and watershed observed data, the surface infiltration process can be modeled as below (Eq. 2) (Liu et al. 2008).

$$f = R \cdot P^r \tag{2}$$

where f is soil infiltration (mm), P is rainfall (mm), and R and r are empirical coefficients which can be obtained by look-up table with land use/land cover and antecedent soil moisture.

In fact, the effective precipitation, which will be available in the process of soil infiltration, is the part of precipitation after interception and lateral supply. A further improvement in our study was attempted to account for the infiltration process. The rainfall in Eq. 2 is replaced with effective precipitation, which is the difference between rainfall and canopy interception (Eq. 3):

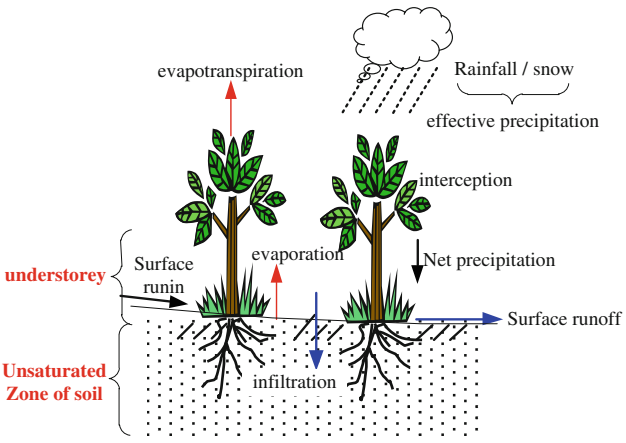

Fig. 4 Sketch map of water cycling process for vegetation under accidented terrain. The *black arrows* denote the water supply source in forest area (rainfall, or surface runoff), and *red and blue arrows* indicate the water export

$$f = R \cdot (P - I)^r \quad (3)$$

in which, I is the canopy interception (mm).

The canopy-intercepted precipitation (I) is disposed as original BEPS, assuming to be proportional to leaf area index (LAI), which is constrained by precipitation (Liu et al. 2003):

$$I = \min(LAI \times b_{\text{int}} \times 10, P) \quad (4)$$

where b_{int} is the precipitation interception coefficient (mm/LAI/day) and LAI is the leaf area index (cm/cm). Daily canopy precipitation interception is calculated and then summed up to 10-day level. The function *min* takes the minimum of the two parameters.

The total water supply source available can be expressed as the sum of effective precipitation and surface runoff coming from neighboring pixels in prior time $t-1$ (Q_{t-1}). So Eq. (3) will be explained as (Eq. 5):

$$f = R \cdot (P - I + Q_{t-1})^r \quad (5)$$

2. Surface runoff

Surface runoff can be expressed as the difference between available water supply source and infiltration according to the water balance equation. In our study, the surface runoff is expressed as:

$$\begin{aligned} Q_t &= (P - I + Q_{t-1}) - f \\ &= (P - I + Q_{t-1}) - R \cdot (P - I + Q_{t-1})^r \end{aligned} \quad (6)$$

where Q_t is surface runoff going out surrounding pixels in current time t.

3. Flowing direction

A window of 3 × 3 pixels was used to calculate the flowing direction based on DEM data. The differences of digital elevation were calculated between the middle pixel and neighboring eight pixels. The maximum difference (filled with diagonals) was chosen as the flowing direction (Fig. 5a). The resulted surface runoff was added into the available water supply source in this pixel in next time step. If the pixel's numbers of the maximum difference were more than one, denotes as N, the surface runoff would be averaged by those pixels equally (Fig. 5b, $N = 2$). The average surface runoff would be added into the available water supply source in this/those diagonal pixel(s) in the next time step.

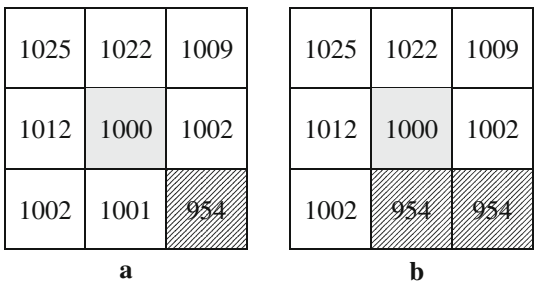

Fig. 5 Determination of flowing direction in a window of 3 × 3 pixels: **a** one maximum difference, and **b** N maximum differences ($N = 2$ in this figure)

Results and discussion

Modeled NPP

Ten-day NPP in Gansu Province, Northwest China in 2003 was modeled using MODIS LAI products (MOD15A2), interpolated meteorological data, and other input parameters based on the modified BEPS. The NPP result was compared with modeled NPP in other studies (Table 1).

We can see that NPP in this study is slightly higher than those in Qinghai-Tibet Plateau and the north piedmont of Tianshan Mountains for forest vegetation. Compared with average NPP of forest vegetation in western China, modeled NPP in this study is lower, while it is in the range of estimated NPP for the whole China. Modeled NPP of grass is comparable to estimated NPP by Zhang and Pan (2010) in the north piedmont of Tianshan Mountains, and higher than the estimation in other studies in Table 1. In terms of crop, modeled NPP in this study is still close to the estimation by Zhang and Pan (2010), slightly higher than that by Sun and Zhu (2000), and lower than that by Liu et al. (2011a) and Lu et al. (2005).

The modeled NPP was further validated using 14 ground measurements through tree ring data in 2003 (Fig. 6). The locations of 14 validation sites are shown in Fig. 2b. Detailed descriptions about measured NPP can be found in the literature written by Zhou et al. (2007). The RMSE (Root Mean Square Error) of modeled NPP are 60.19 and 46.53 gC m^{-2} using original and modified BEPS, respectively. The R^2 between measured and modeled NPP is 0.662 using original BEPS, and it increases to 0.746 using modified BEPS. The findings from this study indicate that the modified BEPS performs better than the original model in NPP modeling in arid and semi-arid region in Northwest China.

NPP of vegetation types

Simulated NPP of different vegetation types were compared for original and modified BEPS. Meanwhile the difference ratio was got with Eq. 7. The results were shown in Table 2.

Table 1 Comparison of modeled NPP (gC m^{-2} a^{-1}) using modified BEPS and other studies

Researcher	Model	Period	Region	Forest	Grass	Crop
Sun and Zhu (2000)	Improve CASA	1992	China	400–972	116–191	313–400
Liu et al. (2011a, b)	CASA	2003-2007	China	446–1,066	219.13	472.62
Piao and Fang (2002)	CASA	1982-1999	Qinghai-Tibet Plateau, China	413.84	176.00	175.00
Lu et al. (2005)	C-FIX	2002	Western China	632.55	172.61	492.00
Zhang and Pan (2010)	NPP-PEM	2002	The north piedmont of Tianshan Mountains	422.57	156–344	375.27
Our study	Modified BEPS	2003	Gansu Province in Northwest China	475.61	283.76	413.95

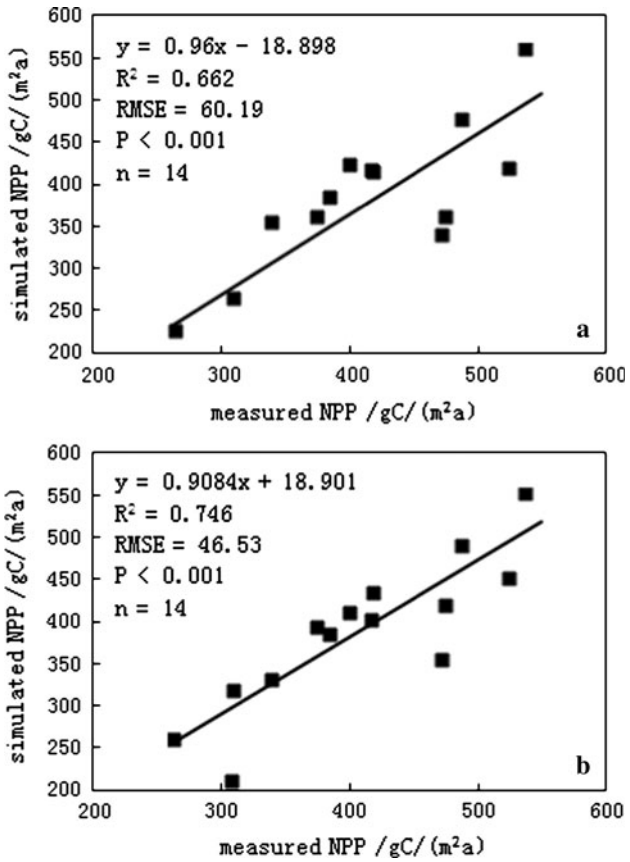

Fig. 6 Comparison between modeled and measured NPP using original (**a**) and modified (**b**) BEPS

$$D_r = \frac{NPP_m - NPP_o}{NPP_o} \times 100\% \quad (7)$$

where NPP_m and NPP_o are simulated NPP with modified and original BEPS, respectively.

The modeled NPP of all vegetation types with modified BEPS are slightly higher than those using the original BEPS (Table 2). The difference of forest NPP is the largest among three vegetation types with a difference ratio of 9.21 %, grass followed by a ratio of 8.10 %, and crop NPP is the lowest with a ratio of 4.29 %. NPP of crop, an irrigative agricultural type, in Gansu Province is influenced hardly by precipitation. This is one of the reasons that the difference ratio of crop NPP is the smallest among three vegetation types. At the same time, smaller runoff at relatively flat terrain may be another reason for smallest NPP difference ratio in some non-irrigated cropland areas. While NPP of natural vegetation, such as forest and grass, are affected largely by precipitation in arid and semi-arid regions with a higher difference ratio of over 8 %.

NPP in five zones

Modeled NPP using modified BEPS was generally higher than that using original BEPS in five zones (Table 3). The largest difference of modeled NPP using original and modified BEPS occurs in the zone of Hexi Corridor and northern Mountain, with ratio up to 14.12 %. In the zone of Hexi Corridor and northern Mountain, annual precipitation is <100 mm. When the surface runoff from neighboring pixels is available for vegetation growth, higher and more accurate vegetation NPP can be modeled using the modified BEPS. The same reason is applicable in the zones of Middle Loess Plateau and Qilian Mountain, where the annual precipitation is <300 mm. In these two zones, the difference ratios of simulated NPP are 7.85 and 7.72 %, respectively. While in the zones of Southern Plateau and Southern Mountain, the difference ratios of simulated NPP are <5.20 % because of their abundant precipitation, which are more than 450 mm.

Spatial distribution

We modeled annual NPP using the modified BEPS in Gansu province from 2002 to 2010, and analyzed the spatial pattern of average NPP over 9-year period (Fig. 7).

The 9-year average NPP of vegetation ranges from 100 to 600 gC m^{-2} a^{-1} in Gansu Province. The NPP displays a decreasing trend from south to north.

It is wet and cold being affected by the Mongolian anticyclone and continental cyclones in Southern Plateau. It has been one of the most important forestry and animal husbandry bases in Gansu Province for its rich forestry resources and vast grasslands. The annual NPP in this zone, which is more than 550 gC m^{-2} a^{-1} in most areas, is

highest among the whole Gansu Province for its abundant precipitation.

The resources of water and forest are abundant in the region of Southern Mountain. The annual NPP of vegetation in this zone is more than 500 gC m^{-2} a^{-1} for its favorable hydrothermal conditions.

Zone of Qilian Mountain is dominated by water conservation forest, and *Picea crassifolia* is the typical vegetation in this zone. Annual NPP of forest ranges from 200 to 600 gC m^{-2} a^{-1} due to the large difference of altitude and dramatic change of temperature.

The annual NPP of vegetation ranges from 150 to 450 gC m^{-2} a^{-1} in Middle Loess Plateau zone, decreasing from south to north and from west to east for its low vegetation coverage and soil nutrient content.

Hexi Corridor and northern Mountains is an irrigation agricultural area and has been a major foodstuff base in Gansu Province. Without considering irrigation in the modified BEPS, the modeled NPP is about 100–300 gC m^{-2} a^{-1}, which may be smaller than the real NPP.

Table 2 Modeled NPP (gC m^{-2} a^{-1}) using original and modified BEPS and their difference ratios (%) for different vegetation types

Vegetation type	NPP using original BEPS	NPP using modified BEPS	Difference ratio (%)
Forest	435.50	475.61	9.21
Grass	382.92	413.95	8.10
Crop	272.10	283.76	4.29

Table 3 Modeled NPP (gC m^{-2} a^{-1}) using original and modified BEPS and their difference ratios (%) in five zones

Zone	NPP using original BEPS	NPP using modified BEPS	Difference ratio (%)
Hexi Corridor and northern Mountains	278.54	317.88	14.12
Middle Loess Plateau	237.18	255.79	7.85
Qilian Mountain	257.17	277.02	7.72
Southern Plateau	585.98	614.17	4.81
Southern Mountain	525.46	552.36	5.12

Seasonal pattern of NPP

Modeled NPP in Gansu province using the modified BEPS model was evaluated in terms of its seasonal patterns (Fig. 8). Twelve months were aggregated to four seasons (3,4,5 for spring, 6,7,8 for summer, 9,10,11 for autumn, and 12,1,2 for winter). The modeled NPP shows significant seasonal pattern in the whole Gansu Province, except Hexi Corridor and northern Mountains due to limited precipitation and low vegetation coverage.

In spring, snow begins to melt and vegetation is gradually growing as temperature rises. Vegetation in southern Mountain grows quickly and the NPP in part of this area reaches to 180 gC m^{-2}. In zone of southern Plateau, NPP ranges from 60 to 180 gC m^{-2}. Vegetation in the zones of Middle Loess Plateau and Qilian Mountain grows slower relatively. The NPP in these two zones are about 20 gC m^{-2} and can reach up to 100 gC m^{-2} in some areas.

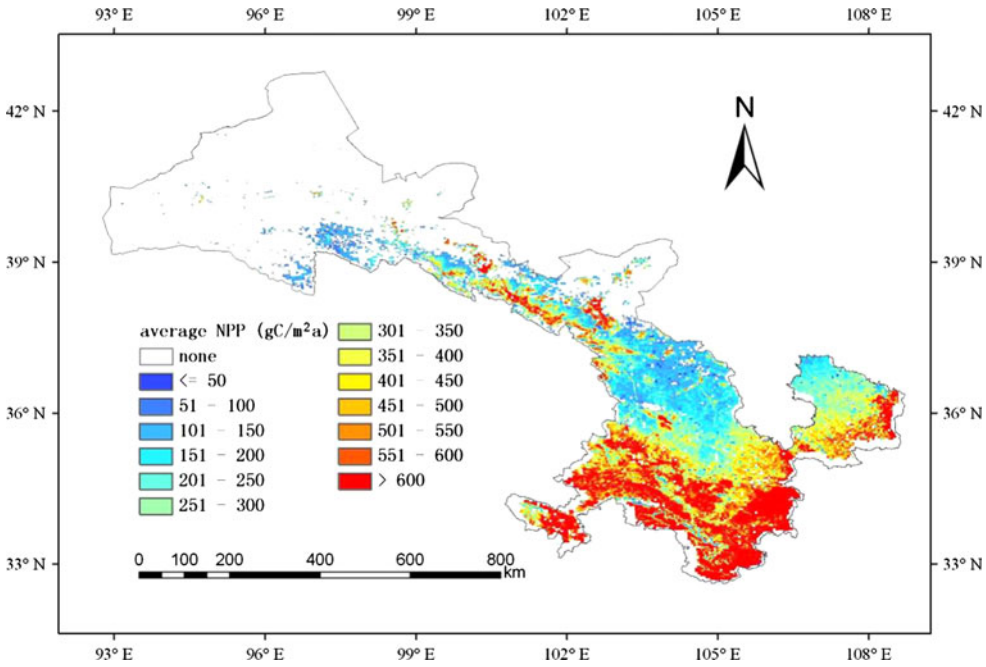

Fig. 7 Spatial distribution of 9-year average NPP in Gansu province

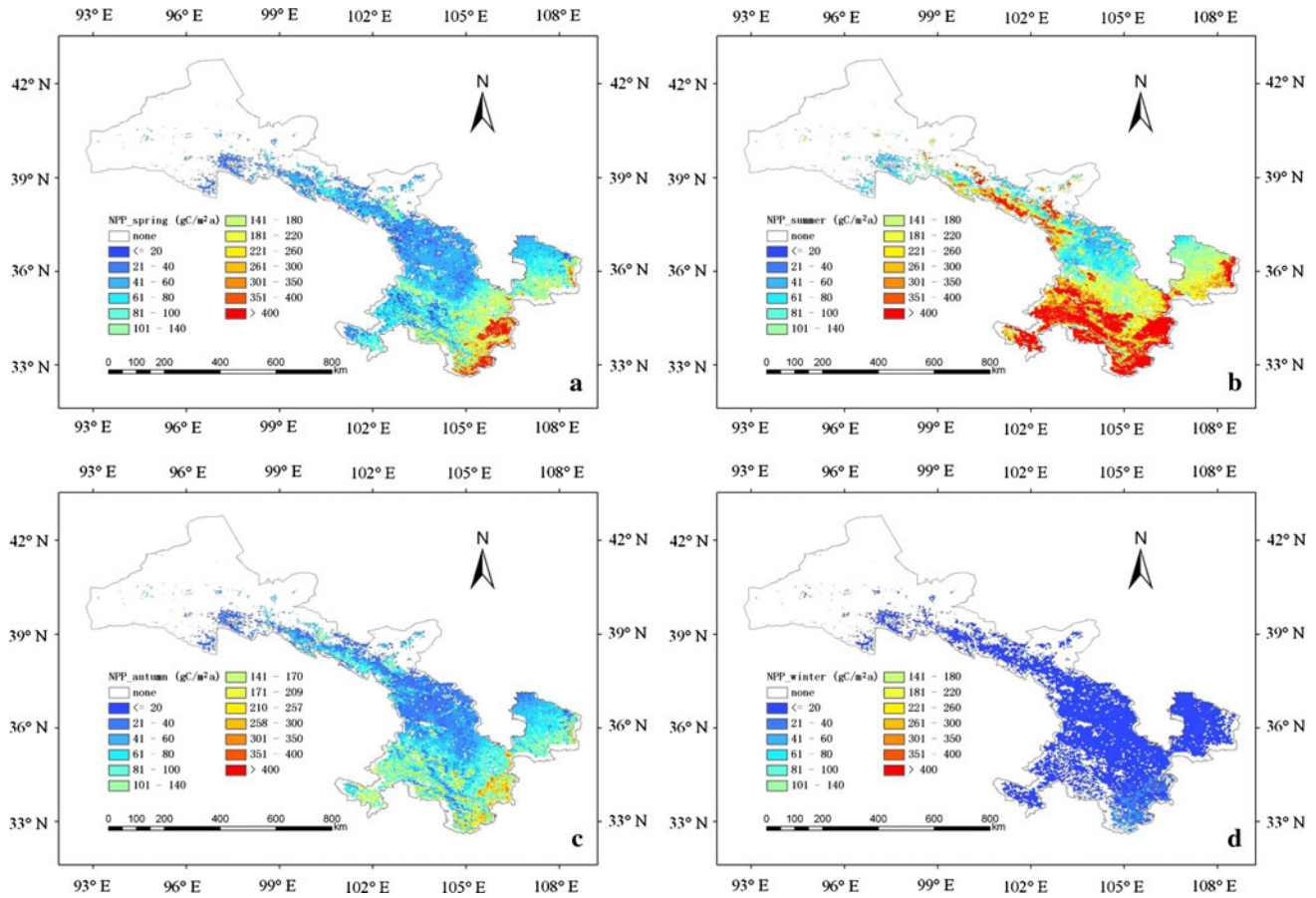

Fig. 8 Seasonal NPP of vegetation in Gansu province (**a** spring, **b** summer, **c** autumn, and **d** winter)

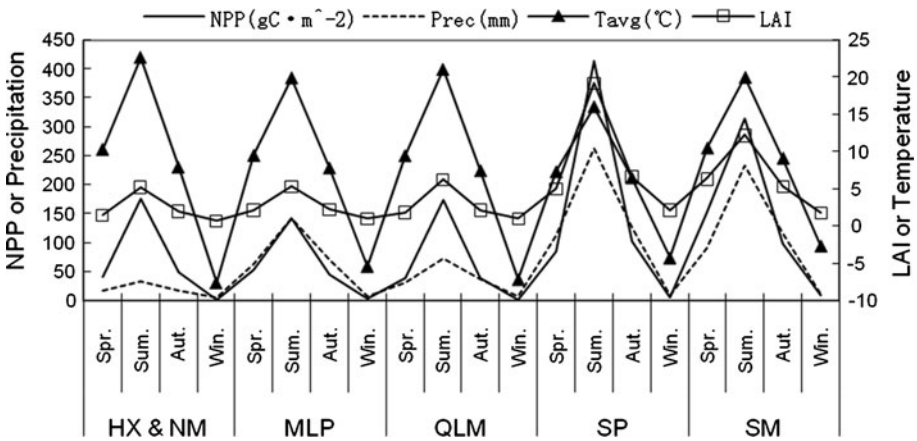

Fig. 9 Modeled NPP and its key drivers in four seasons and five zones. The *HX & NM* denote Hexi Corridor and northern mountain, *MLP* denotes Middle Loess Plateau, *QLM* denotes Qilian Mountain, *SP* denotes Southern Plateau, and *SM* is Southern Mountain

The growth rate of vegetation speeds up for its abundant thermal and hydrological resources in summer. The fast growth zones concentrate in Qilian Mountain, southern Mountain, and southern Plateau. Vegetation NPP in those zones reach to 200 gC m^{-2} and even more than 400 gC m^{-2} in the summer time. NPP in Middle Loess Plateau, Hexi Corridor, and northern Mountains in the summer time can reach to 100 gC m^{-2}.

In autumn, as the temperature and precipitation decrease, vegetation growth rate slows down. NPP is <260 gC m^{-2} in the whole Gansu Province in the autumn time. The remarkable reduction of NPP occurs in zones of southern Mountain, southern Plateau, and Qilian Mountain, where NPP decrease to 80–260 gC m^{-2}, compared with the summer time. In Middle Loess Plateau, Hexi Corridor, and northern Mountains, NPP decrease to <80 gC m^{-2} with the crops harvest.

NPP in winter is low (<5 gC m^{-2}) in most parts of Gansu province because of low temperature. Only in some areas of southern Mountain, NPP is close to 5–20 gC m^{-2}.

Seasonal NPP of vegetation and its key impact factors, including seasonal temperature, total precipitation, and average LAI, in five zones are shown in Fig. 9. The seasonal trends of NPP and LAI in five zones are apparent with high values in summer and low values in winter, so are seasonal temperature, precipitation, and LAI.

Conclusions

In this study, the BEPS model is improved to simulate the NPP of vegetation in arid and semi-arid region in Northwest China. In order to better understand the impact of the characteristics of geography and climate on NPP simulation, the processes of infiltration and surface runoff were introduced into water cycling sub-model in the BEPS. NPP in Gansu Province, Northwest China was modeled using the modified BEPS at moderate spatial resolution from 2002 to 2010. The spatial pattern of modeled NPP shows that high values centralized in the high altitude areas with growing forest and grassland, and the low NPP generally distributed in Hexi Corridor and Northern Mountains with its sparse vegetation coverage. Meanwhile, evident seasonal trend of modeled NPP was found with high NPP in summer and low value in winter.

The findings in this study indicates that three-dimension hydrological model, especially the processes of infiltration and surface runoff, should be considered to accurately model the vegetation NPP in arid and semi-arid regions. In the case of this study, when modeling NPP in area with large variation of elevation, ground water hydrology cannot be ignored for better understanding of its contributions to vegetation growth.

In this paper, although we modeled NPP for all types of vegetation in the study area, only NPP of forest was validated using ground measurements due to data availability. More work should be done in the future to acquire more field measurements not only in larger spatial ranges but also for more vegetation types, which will be helpful to model the NPP of different vegetation types in arid and semi-arid regions more scientifically and reasonably. Further validation for all vegetation types will help us to obtain a more complete picture of the spatial pattern of NPP, especially in the area with mixed vegetation types.

Another thing is that irrigation was not considered due to the lack of irrigation data when modeling NPP of crop. To improve the NPP modeling of crop in arid and semi-arid regions, information of farm management, including irrigation time, amount, and frequency, needs to be collected in the future. Thus, water cycling sub-model can be improved further by adding irrigation information in the irrigative agricultural area.

Acknowledgments We would like to thank Prof. J. Chen and his group in affording the initial BEPS model. We also gratefully acknowledge the anonymous reviewers for their valuable comments on the manuscript. The study was funded by the National Natural Science Foundation of China (No. 40901170 and 41071224), the Basic Research and Operating Expenses of CAMS (No. 2010Y004), and the National Basic Research Program of China (No. 2010CB951304).

References

Chen JM, Liu J, Cihlar J, Guolden ML (1999) Daily canopy photosynthesis model through temporal and spatial scaling for remote sensing application. Ecol Model 124:99–119

Chen JM, Chen XY, Ju WM, Geng XJ (2005) Distribution hydrological model for mapping evapotranspiration using remote sensing inputs. J Hydrol 305:15–39

Chen XF, Chen JM, An SQ, Ju WM (2007) Effects of topography on simulated net primary productivity at landscape scale. J Environ Manage 85:585–596

Feng XF, Liu GH, Chen JM, Chen MZ, Liu J, Ju WM, Sun R, Zhou WZ (2007) Net primary productivity of China's terrestrial ecosystem from a process model driven by remote sensing. J Environ Manage 85:563–573

Foley JA, Prentice IC, Ramankutty N, Levis S, Pollard D, Sitch S, Haxeltine A (1996) An integrated biosphere model of land surface processes, terrestrial carbon balance, and vegetation dynamics. Global Biogeochem Cycles 10(4):603–628

Hunt ER Jr, Running SW (1992) Simulated dry matter yields for aspen and spruce stand in the North American Boreal Forest. Can J Remote Sensing 18:126–133

Ju WM, Chen JM, Black TA, Barr AG, Liu J, Chen BZ (2006) Modelling multi-year coupled carbon and water flues in a boreal aspen forest. Agric For Meteorol 140:136–151

Leith H, Whittaker RH (1975) Primary productivity of the biosphere. Springer-Verlag, New York

Liu MG (2010) Atlas of physical geography of China. SinoMaps Press, Beijing

Liu J, Chen JM, Cihlar J, Park W (1997) A process—based boreal ecosystem productivity simulator using remote sensing inputs. Remote Sens Environ 62:158–175

Liu J, Chen JM, Cihlar J, Chen W (1999) Net primary productivity distribution in the boreal region from a process model using satellite and surface data. J Geophys Res 104(D22):27735–27754

Liu J, Chen JM, Cihlar J, Chen W (2002) Net primary productivity mapped for Canada at 1-km resolution. Glob Ecol Biogeogr 11:115–129

Liu J, Chen JM, Cihlar J (2003) Mapping evapotranspiration based on remote sensing: an application to Canada's landmass. Water Resour Res 39(7):1189–1203

Liu CM, Wang ZG, Zhen HX, Zhang L, Wu XF (2008) Development and applications of HIMS system and its modules. Scientia Sinica Technologica 38(3):350–360 (in Chinese)

Liu JF, Xiao WF, Guo CM, Wu HP, Jiang ZP (2011a) Pattern analysis of net primary productivity of China terrestrial vegetation using 3-PGS model. Scientia Silvae Sinicae 47(5):16–22 (in Chinese with English abstract)

Liu X, He B, Li Z, Zhang J, Wang L, Wang Z (2011b) Influence of land terracing on agricultural and ecological environment in the loess plateau regions of China. Environ Earth Sci 62:797–807

Lu L, Li X, Veroustraete F (2005) Terrestrial net primary productivity and its spatial-temporal variability in western China. Acta Ecologica Sinica 25(5):1026–1032 (in Chinese with English abstract)

Matsushita B, Tamura M (2002) Integrating remotely sensed data with an ecosystem model to estimate net primary productivity in East Asia. Remote Sens Environ 81(1):58–66

Matsushita B, Xu M, Chen J, Kameyama S, Tamura M (2004) Estimation of regional net primary productivity (NPP) using a process-based ecosystem model: how important is the accuracy of climate data? Ecol Model 178:371–388

Piao SL, Fang JY (2002) Terrestrial net primary production and its spatio-temporal patterns in Qinghai-Xizang Plateau, China during 1982–1999. J Nat resour 17(3):373–380 (in Chinese with English abstract)

Potter CS, Randerson JT, Field CB, Matson PA, Vitousek PM, Mooney HA, Kloster SA (1993) Terrestrial ecosystem production: a process model based on global satellite and surface data. Global Biogeochem Cycles 7(4):811–841

Running SW, Coughlan JC (1988) A general model of forest ecosystem processes for regional applications I. Hydrologic balance, canopy gas exchange and primary production processes. Ecol Model 42:125–154

Soulis ED, Snelgrove KR, Kouwen N, Seglenieks F, Verseghy DL (2000) Towards closing the vertical water balance in Canadian atmospheric models: coupling of the land surface scheme class with the distributed hydrological model watflood. Atmos Ocean 38:251–269

Sun R, Zhu QJ (2000) Distribution and seasonal change of net primary productivity in China from April, 1922 to March, 1993. Acta Geographica Sinica 55(1):36–45 (in Chinese with English abstract)

Wang PJ, Sun R, Zhu QJ, Xie DH, Chen JM (2006) Improvement on the abilities of BEPS under accidented terrain. J Imag Gr 11(7):1017–1025 (in Chinese with English abstract)

Wang PJ, Sun R, Hu JC, Zhu QJ, Zhou YY, Li L, Chen JM (2007) Measurements and simulation of forest leaf area index and net primary productivity in Northern China. J Environ Manage 85:607–615

Wang B, Yang S, Lv C, Zhang J, Wang Y (2010) Comparison of net primary productivity in karst and non-karst areas: a case study in Guizhou Province, China. Environ Earth Sci 59:1337–1347

Winslow JC, Hunt ER, Piper SC (2001) A globally applicable model of daily solar irradiance estimated from air temperature and precipitation data. Ecol Model 143:227–243

Zhang J, Pan XL (2010) Spatial pattern and seasonal dynamics of net primary productivity in mountain—oasis—desert ecosystem on the north piedmont of Tianshan Mountains in arid north-west China. Arid Land Geography 33(1):78–86 (in Chinese with English abstract)

Zhang Y, Zhou G (2011) Exploring the effects of water on vegetation change and net primary productivity along the IGBP Northeast China Transect. Environ Earth Sci 62:1481–1490

Zhang KK, Bu CF, Gao GX (2011) Effect of microbiotic crust on soil water infiltration in the loess plateau. Arid Zone Res 28(5):808–812 (in Chinese with English abstract)

Zhou WZ, Liu GH, Pan JJ, Feng XF (2005) Distribution of available soil water capacity in China. J Geog Sci 15(1):3–12

Zhou YY, Zhu QJ, Chen JM, Wang YQ, Liu J, Sun R (2007) Observation and simulation of net primary productivity in Qilian Mountain, western China. J Environ Manage 85:574–584

Zhou X, Yan Y, Wang H, Zhang F, Wu L, Ren J (2011) Assessment of eco-environment vulnerability in the northeastern margin of the Qinghai-Tibetan Plateau, China. Environ Earth Sci 63:667–674